

Learning to Solve Large-Scale Security-Constrained Unit Commitment Problems

Álinson S. Xavier¹, Feng Qiu¹, and Shabbir Ahmed²

¹ Energy Systems Division, Argonne National Laboratory, Argonne, IL, USA. {axavier,fqiu}@anl.gov

² School of Industrial and Systems Engineering, Georgia Institute of Technology, Atlanta, GA, USA.

sahmed@isye.gatech.edu

Abstract. Security-Constrained Unit Commitment (SCUC) is a fundamental problem in power systems and electricity markets. In practical settings, SCUC is repeatedly solved via Mixed-Integer Linear Programming, sometimes multiple times per day, with only minor changes in input data. In this work, we propose a number of machine learning (ML) techniques to effectively extract information from previously solved instances in order to significantly improve the computational performance of MIP solvers when solving similar instances in the future. Based on statistical data, we predict redundant constraints in the formulation, good initial feasible solutions and affine subspaces where the optimal solution is likely to lie, leading to significant reduction in problem size. Computational results on a diverse set of realistic and large-scale instances show that, using the proposed techniques, SCUC can be solved on average 12 times faster than conventional methods, with no negative impact on solution quality.

Keywords: Security-Constrained Unit Commitment · Mixed-Integer Linear Programming · Machine Learning

1 Introduction

Security-Constrained Unit Commitment (SCUC) is one of the most fundamental optimization problems in power systems and electricity markets, being solved a number of times daily by major reliability coordinators, independent system operators (ISOs), and regional transmission organizations (RTOs) to schedule 3.8 trillion kWh of energy production and clear a \$400 billion electricity market annually in the United States (EIA, 2018). The problem asks for the most cost-efficient schedule for power generation units under a large number of physical, operational and economic constraints. Among other requirements, a feasible generation schedule must not only guarantee that enough power is being produced during each hour to satisfy the demand, but also that no transmission lines are overloaded during the delivery of the electric power. Furthermore, the schedule must be robust against small variations in demands and against the unexpected loss of a small number of network elements, such as generation units and transmission lines.

The computational performance of SCUC is an extremely important practical issue, given the very short clearing windows enforced in most electricity markets. For instance, in Midcontinent Independent System Operator (or MISO, the largest electricity market in North America), systems operators only have 3 or 4 hours, after receiving all bids and offers, to produce a low-cost and fair generation schedule. During this short time window, SCUC must be solved multiple times, under a number of different scenarios. Using state-of-art software, realistic large-scale instances can be usually solved to 0.1% optimality within approximately 20 minutes of running time (Chen et al., 2016). Improvements in computational performance would allow markets to implement numerous enhancements that could bring significant economic benefits and improved market efficiency, such as more accurate modelling of enhanced combined cycle units, higher resolution for production cost curves, sub-hourly dispatch, longer planning horizons, among others. Alternatively, a simple reduction of the optimality gap to 0.05% without sacrificing computational running times could lead to significant cost savings, considering the \$400 billion market size in U.S. alone. In the past, SCUC has been solved using various optimization techniques including priority lists (Burns and Gibson, 1975), dynamic programming (Lowery, 1966) and Lagrangian relaxation (Merlin and Sandrin, 1983). Nowadays, SCUC is most commonly formulated as a Mixed-Integer Linear Programming (MIP). The introduction of MIP solvers allowed system operators to easily model more realistic constraints that had been traditionally hard to enforce with previous methods, and have benefited from the constantly advancing capabilities of modern solvers. Since the first MIP formulations, proposed in the 1960s (Garver, 1962), a number of alternative formulations and polyhedral results have been described (Atakan et al., 2018; Ostrowski et al., 2012; Rajan et al., 2005; Gentile et al., 2017; Damci-Kurt et al., 2016; Morales-España et al., 2015; Lee et al., 2004; Pan and Guan, 2016; Knueven et al., 2018). There has also been active research on more practical techniques for improving the computational performance of the MIP approach, such as fast identification of redundant constraints (Zhai et al., 2010; Ardakani and Bouffard, 2015; Xavier et al., 2019), decomposition methods (Feizollahi et al., 2015; Kim et al., 2018), among others.

One aspect of SCUC that has been overlooked in previous research is that, in most practical settings, this problem is repeatedly solved with only minor changes in input data, often multiple times per day. Most of the system characteristics, such as the parameters describing the generation units or the topology of the transmission network, are kept almost entirely unchanged from solve to solve. While modern MIP solvers have the ability to reuse previous solutions as warm starts, it is well known that, for SCUC, providing the previous-day

optimal solution brings only minor performance improvements (Chen et al., 2016). In this work, we propose the use of machine learning to effectively extract information from previously solved instances, and show how to leverage this information to significantly accelerate the solution of similar instances in the future.

Machine learning (ML) is a discipline that studies how algorithms can automatically learn from large amounts of data and subsequently use the acquired knowledge to make decisions quickly and accurately. In the 1990s and early 2000s, researchers experimented using artificial neural networks (ANN) to solve simpler variants of SCUC on small-scale instances (Sasaki et al., 1992; Wang and Shahidehpour, 1993; Walsh and O’malley, 1997; Liang and Kang, 2000). Even when considering very simplified versions of the problem, obtaining sufficiently high-quality solutions to SCUC via ANN proved very challenging, and the approach failed to replace existing methods. Similar explorations with evolutionary algorithms proved equally challenging (Juste et al., 1999). In more recent years, there has been a growing interest, within the broader mathematical optimization community, in applying ML techniques to enhance the performance of current MIP solvers. For instance, ML has been used to automatically construct branching strategies (Alvarez et al., 2017; Khalil et al., 2016), to better parallelize branch-and-bound methods (Alvarez et al., 2014), and to decide when to run primal heuristics (Khalil et al., 2017). See (Lodi and Zarpellon, 2017) for a survey on these methods.

In this work, instead of completely replacing existing MIP methods by ML models, as done in previous research with artificial neural networks and genetic algorithms, we propose the usage of ML techniques to significantly enhance the warm-start capabilities of modern MIP solvers when solving SCUC. More specifically, we develop three ML oracles that can automatically identify different types of patterns in previously solved instances and subsequently use these patterns to improve MIP performance. The first oracle is designed to predict, based on statistical data, which constraints are necessary in the formulation and which constraints can be safely omitted. The second oracle identifies, among a large number of previously obtained optimal solutions, which ones are likely to work well as MIP starts. The third oracle identifies, with very high confidence, a smaller-dimensional affine subspace where the optimal solution is likely to lie, leading to the elimination of a large number of decision variables and significantly reducing the complexity of the problem.

We start, in Section 2, by introducing the MIP formulation of this problem. In Section 3, we formalize the setting in which the learning takes place and we describe the proposed learning strategies. Finally, in Section 4, we evaluate the practical impact of the proposed ML approach by performing extensive computational experiments on a diverse set of large-scale

and realistic SCUC instances, containing up to 6515 buses and 1388 units, under realistic uncertainty scenarios. Using the proposed technique, we show that SCUC can be solved on average 12 times faster than conventional methods, with no negative impact on solution quality. The techniques presented are very general, and can be easily adapted to other challenging optimization problems.

2 The Security-Constrained Unit Commitment Problem

Unit Commitment (UC) refers to a broad class of optimization problems dealing with the scheduling of power generating units (Cohen and Sherkat, 1987). For each hour in the planning horizon, the problem is to decide which units should be operational and how much power should they produce (Ostrowski et al., 2012). Each unit typically has minimum and maximum power outputs, a quadratic production cost curve, and fixed startup and shutdown costs. Other constraints typically include ramping rates, which restrict the maximum variation in power production from hour to hour, and minimum-up and minimum-down constraints, which prevents units from starting and shutting down too frequently. The Security-Constrained Unit Commitment (SCUC) problem is a subclass of UC that, in addition to all the constraints previously mentioned, also guarantees the deliverability of power, by enforcing that the power flow in each transmission line does not exceed its safe operational limits (Shaw, 1995). To guarantee sufficient security margin in case of component failure, the problem considers not only transmission constraints under normal operating conditions, but also when there is one transmission line failure in the system (so-called N-1 transmission contingency) (Batut and Renaud, 1992). In this way, even if a transmission line unexpectedly fails and the power flow in the network changes, there will be no violations of the transmission line thermal limits.

A number of MIP formulations and strong valid inequalities for SCUC have been proposed. In this work, we use the formulation proposed in (Morales-España et al., 2013), since it presents good computational performance even when transmission and N-1 security constraints are present. The full MIP formulation is shown in Appendix A. Here, we present a simplified summary, containing key decision variables and constraints that are most influential to the computational performance of the problem. Consider a power system composed by a set B of buses, a set G of generators and a set L of transmission lines. Let T be the set of hours within the planning horizon. For each generator $g \in G$ and hour $t \in T$, let x_{gt} be a binary decision variable indicating if the generator is operational, and y_{gt} be a continuous decision variable

indicating the amount of power being produced. The problem can then be formulated as

$$\text{minimize} \quad \sum_{g \in G} c_g(x_{g\bullet}, y_{g\bullet}) \quad (1)$$

$$\text{subject to} \quad (x_{g\bullet}, y_{g\bullet}) \in \mathcal{G}_g \quad \forall g \in G \quad (2)$$

$$\sum_{g \in G} y_{gt} = \sum_{b \in B} d_{bt} \quad \forall b \in B, t \in T \quad (3)$$

$$-F_l^0 \leq \sum_{b \in B} \delta_{lb}^0 \left(\sum_{g \in G_b} y_{gt} - d_{bt} \right) \leq F_l^0 \quad \forall l \in L, t \in T. \quad (4)$$

$$-F_l^c \leq \sum_{b \in B} \delta_{lb}^c \left(\sum_{g \in G_b} y_{gt} - d_{bt} \right) \leq F_l^c \quad \forall c \in L, l \in L, t \in T. \quad (5)$$

$$x_{gt} \in \{0, 1\} \quad \forall g \in G, t \in T \quad (6)$$

$$y_{gt} \geq 0 \quad \forall g \in G, t \in T \quad (7)$$

In the objective function, c_g is a piecewise-linear function which includes the startup, shutdown and production costs for generator g . The notation $(x_{g\bullet}, y_{g\bullet})$ is a shorthand for the vector $(x_{gt_1}, \dots, x_{gt_k}, y_{gt_1}, \dots, y_{gt_k})$, where $\{t_1, \dots, t_k\} = T$. Constraint (2) enforces a number of constraints which are local for each generator, including production limits and ramping rates. Constraint (3) enforces that the total amount of power produced equals the sum of the demands d_{bt} at each bus. Constraints (4) enforce the deliverability of power under normal system conditions. The set G_b denotes the set of generators attached to bus b . We recall that power flows are governed by physical laws, i.e., Ohm's laws and Kirchhoff's Laws. Using the DC linearization of these laws, it is possible to express the thermal limits for each transmission line as (4), where δ_{bl}^0 are real numbers known as injection shift factors. Similarly, constraints (5) enforce the deliverability of power under the scenario that line c has suffered an outage. Note that the bounds and the injection shift factors may be different under each outage scenario.

To improve the strength of the linear relaxation, the full formulation contains additional auxiliary binary decision variables. However, once x_{gt} is determined, all the other binary variables are immediately implied. Furthermore, once all the x_{gt} variables are fixed, the problem reduces to a linear programming problem (known as Economic Dispatch) which can be solved efficiently.

Constraints (4) and (5) have a significant impact on the computational performance of SCUC. The total number of such constraints is quadratic on the number of transmission lines. Since large power systems can have more than 10,000 lines, the total number of constraints

can easily exceed hundreds of millions. To make matters worse, these constraints are typically very dense. Adding them all to the formulation not only leads to significant performance degradation, but also to out-of-memory errors. Fortunately, it has been observed that enforcing only a very small subset of these constraints is already sufficient to guarantee that all the remaining ones are automatically satisfied (Bouffard et al., 2005). Identifying this critical subset of constraints can be very challenging, and usually involves either solving a relaxation of SCUC multiple times (Tejada-Arango et al., 2018; Xavier et al., 2019) or solving auxiliary optimization problems (Ardakani and Bouffard, 2015; Zhai et al., 2010). In practice, system operators still rely on experience and external processes to pre-select a subset of constraints to include in the optimization problem.

Based on the previous remarks, in the next sections we focus on developing ML oracles to predict the values of the x_{gt} variables and to predict which transmission constraints can be omitted from the formulation.

3 Setting & Learning Strategies

In this section, we formalize the setting in which the learning takes place, in addition to our proposed learning strategies. The theoretical setting below was designed to match the realistic conditions that energy market operators face on a daily basis.

Assume that every instance $I(p)$ of SCUC is completely described by a vector of real-valued parameters p . These parameters include only the data that is unknown to the market operators the day before the market clearing process takes places. For example, they may include the peak system demand and the production costs for each generator. Since the network topology and the total number of generators is known in advance, there is no need to encode them via parameters. We may, therefore, assume that $p \in \mathbb{R}^n$, where n is fixed. Although the precise value of each parameter is uncertain, we assume that their joint probability distribution is known in advance. This is not an unrealistic assumption, since market operators have been solving SCUC daily for years and have terabytes of accumulated data which can be analyzed.

We also assume that we have at our disposal a customized MIP solver which can receive, in addition to the instance $I(p)$ to be solved, a vector of hints. These hints may affect the performance of the MIP solver and will, hopefully, improve its running time. The hints may also affect the quality or optimality of the solutions produced by the MIP solver. Examples of hints may include a list of MIP starts, a list variables that should be fixed, or a list of initial constraints to enforce.

During the training phase, our task is to construct an oracle ϕ which maps each possible parameter $p \in \mathbb{R}^n$ into a vector of hints. In order to build this oracle, we are allowed to take samples from the joint probability distribution, construct training instances of the problem and solve them to optimality, capturing any data we may consider useful. During the test phase, one particular vector of parameters \tilde{p} is sampled from the distribution, the vector of hints $\phi(\tilde{p})$ is computed and the pair $(I(\tilde{p}), \phi(\tilde{p}))$ is given to the MIP solver. The total running time is measured, including the time taken to construct the vector of hints from the parameters, as well as the time taken by the MIP solver to solve the instance.

In the following, we propose three different oracles, which target different challenges of solving SCUC. The first oracle is focused on predicting violated transmission and N-1 security constraints. The second oracle focuses on producing initial feasible solutions, which can be used as MIP starts. The third oracle aims at predicting an affine subspace where the solution is likely to lie.

3.1 Learning violated transmission constraints

As explained in Section 2, one of the most complicating factors when solving SCUC is handling the large number of transmission and security constraints that need to be enforced. Our first oracle is designed to predict which transmission constraints should be added to the relaxation and which constraints can be safely omitted based on statistical data. We also show how the iterative contingency screening algorithm presented in (Xavier et al., 2019) can be modified to work with these hints. Let L be the set of transmission lines. We recall that each transmission constraint takes the form

$$-F_l^c \leq \sum_{b \in B} \delta_{lb}^c \left(\sum_{g \in G_b} y_{gt} - d_{bt} \right) \leq F_l^c \quad \forall l \in L, c \in L \cup \{0\}, t \in T.$$

We assume that the customized MIP solver accepts, from the transmission oracle, a vector of hints

$$h_{l,c,t} \in \{\text{ENFORCE, RELAX}\} \quad \forall l \in L, c \in L \cup \{0\}, t \in T,$$

indicating whether the thermal limits of transmission line l , under contingency scenario c , at time t , is likely to be binding in the optimal solution. Given these hints, a modified version of the iterative algorithm presented in (Xavier et al., 2019) can be constructed as follows. In the first iteration, only the transmission constraints specified by the hints are enforced. A solution is obtained, the thermal limits for all transmission lines are verified, then a small subset of violated constraints are added to the relaxation. The procedure repeats until no

more violations are found. For completeness, a complete description of the modified algorithm is presented in Algorithm 1. See (Xavier et al., 2019) for more details on this iterative method (without the ML component). Note that, if the oracle is successful and correctly predicts a superset of the binding transmission constraints, then only one iteration is necessary for the algorithm to converge. This superset, however, should not be too large, since the inclusion of too many transmission constraints during the first iteration of the procedure may significantly slow down the solution time.

Algorithm 1 Security-Constrained Unit Commitment

- 1: Create a relaxation of SCUC without constraints (4) or (5).
- 2: Query transmission oracle and receive vector of hints h .
- 3: **for** $(l, c, t) \in L \times (L \cup \{0\}) \times T$ **do**
- 4: If $h_{l,c,t} = \text{ENFORCE}$, add corresponding constraint (4) or (5).
- 5: Solve the current relaxation.
- 6: **for** $(l, c, t) \in L \times (L \cup \{0\}) \times T$ **do**
- 7: Let $f_{lt}^c = \sum_{b \in B} \delta_{lb}^c \left(\sum_{g \in G_b} y_{gt} - d_{bt} \right)$.
- 8: Let $\gamma_{lt}^c = \max\{-f_{lt}^c - F_l^c, 0, f_{lt}^c - F_l^c\}$.
- 9: Let $\Gamma = \{(l, c, t) \in L \times (L \cup \{0\}) \times T : \gamma_{lt}^c > 0\}$ be set of violated constraints.
- 10: **if** Γ is empty **then return** current solution.
- 11: **else**
- 12: For every $l \in L, t \in T$, keep in Γ only the pair (l, c, t) with highest γ_{lt}^c .
- 13: For every $t \in T$, keep in Γ only the 15 pairs (l, c, t) having the highest γ_{lt}^c .
- 14: For every violation in Γ , add the corresponding constraint to the relaxation.
- 15: **goto** step 5.

Based on experimental observations, we propose a very simple learning strategy for the transmission oracle. First, multiple training instances are generated and each one is solved using Algorithm 1, where the initial hints are set to $h_{l,c,t} = \text{RELAX}$ for all constraints. During test phase, the oracle returns $h_{l,c,t} = \text{ENFORCE}$ if the transmission constraint (l, c, t) was necessary during the solution of at least k percent of the training samples, where k is a fixed hyperparameter. That is, the oracle accumulates the entire list of transmission constraints that were ever necessary during training, and outputs a subset that appeared frequently, where the parameter k is specified by the user. In our experiments, this parameter was set to 1%. While, in principle, this strategy could lead to a very large number of transmission constraints being added to the initial relaxation, we have observed that, under realistic parameter distributions, this subset remains relatively small, even for power systems of very large size. Furthermore, it is very effective at reducing the number of iterations.

We also note that this transmission oracle is very suitable for online learning, and can be used even when only a very small number of training samples is available. After a few training samples has been solved, subsequent training can already use hints derived from these samples.

3.2 Learning initial feasible solutions

Another considerably challenging aspect of solving large-scale SCUC instances is obtaining high-quality initial feasible solutions to the problem. Over the last decades, researchers have proposed a number of strong mixed-integer linear programming formulations for SCUC, leading to very strong dual bounds being obtained fairly quickly during the optimization process. For challenging instances, however, we have observed that a significant portion of the running time is usually spent in finding a feasible solution that has an objective value close to this dual bound. These solutions are usually found through generic primal heuristics included in the MIP solver, such as feasibility pump (Fischetti et al., 2005) or large neighborhood search (Shaw, 1998).

Our second oracle is designed to quickly produce high-quality valid solutions for SCUC. Here, we propose an instance-based learning approach. First, multiple training instances $I(p^1), \dots, I(p^s)$ are generated, based on the joint probability distribution of the parameters. The optimal solutions $(x^1, y^1), \dots, (x^s, y^s)$ are then computed and stored. During test, given a vector of parameters \tilde{p} , the oracle finds a list of k vectors of parameters p^{i_1}, \dots, p^{i_k} which are the closest to \tilde{p} , under a pre-specified norm, and returns x^{i_1}, \dots, x^{i_k} . The customized MIP solver then uses these k vectors as MIP starts.

While, in principle, the entire list of solutions $(x^1, y^1), \dots, (x^s, y^s)$ could be provided as MIP starts to the solver, we recall that processing each MIP start may still take a non-negligible amount of time. This is specially true since, in order to maximize the likelihood of a MIP start being useful, we only provide values for the integer variables and let the solver find the values for the continuous variables y . Therefore, the solver needs to solve a linear programming problem for each MIP start, which may take significant time when the number of MIP starts is very large. In our experiments, k was set to three, and the infinity norm was used since it presented slightly better performance than others. We also recall that, prior to computing the distance between the parameters, the vectors need to be preprocessed and rescaled, in order to avoid assigning too much importance to vector components that happen to have larger magnitudes.

Like the transmission oracle presented previously, this warm-start oracle is also very suitable for online learning, and can be used with a very small number of training samples.

3.3 Learning affine subspaces

Through their experience, market operators have naturally learned a number of patterns in the optimal solutions of their own power systems. For example, they know that certain power generating units (known as *base units*) will almost certainly be committed throughout the day, while other units (known as *peak units*) typically come online only during peak demand. These and many other intuitive patterns, however, are completely lost when SCUC is translated into a mathematical problem. Given the fixed characteristics of a particular power system and a realistic parameter distribution, new constraints could probably be safely added to the MIP formulation of SCUC to restrict its solution space without affecting its set of optimal solutions. In this subsection, we develop an oracle for finding such constraints automatically, based on statistical data.

More precisely, let \tilde{p} be a vector of parameters. Our goal is to develop an oracle which predicts a list of hyperplanes $(h^1, h_0^1), \dots, (h^k, h_0^k)$ such that, with very high likelihood, the optimal solution (x, y) of $I(\tilde{p})$ satisfies $\langle h^i, x \rangle = h_0^i$, for $i = 1, \dots, k$. For computational reasons, we restrict ourselves to hyperplanes that can be written as

$$x_{gt} = 0, \tag{8}$$

$$x_{gt} = 1, \tag{9}$$

$$x_{gt} = x_{g,t+1}, \tag{10}$$

where $g \in G$ and $t \in T$. In other words, the oracle tries to determine whether each variable x_{gt} should be fixed to zero, to one, or to the next variable $x_{g,t+1}$. Furthermore, to prevent conflicting assignments the oracle makes at most one of these three recommendations for each variable $x_{g,t}$.

Let \mathcal{H} be the set of all hyperplanes considered for inclusion. During the training phase, our goal is to construct, for each hyperplane $(h, h_0) \in \mathcal{H}$, an oracle function $\phi_{(h,h_0)} : \mathbb{R}^n \rightarrow \{\text{ADD, SKIP}\}$, which receives a vector of parameters $\tilde{p} \in \mathbb{R}^n$ and returns the label **ADD** to indicate that the equality constraint $\langle h, x \rangle = h_0$ is very likely to be satisfied at the optimal solution, and **SKIP** otherwise. Given these hints, our customized MIP solver simply adds to the relaxation all the equality constraints $\langle h, x \rangle = h_0$ such that $\phi_{(h,h_0)} = \text{ADD}$. These constraints are added at the very beginning of the optimization process and kept until a solution is obtained. While, in principle, adding these constraints could lead to suboptimal solutions, in

our computational experiments we have observed that, by using a reasonably large number of training samples and by carefully constructing high-precision oracles, as described in detail below, this strategy does not lead to any noticeable degradation in solution quality, while providing significant speedups.

Next we describe how such high-precision oracles can be constructed. Let $(h, h_0) \in \mathcal{H}$. Furthermore, let $I(p^1), \dots, I(p^s)$ be the training instances and let $(x^1, y^1), \dots, (x^s, y^s)$ be their respective optimal solutions. For every $i \in \{1, \dots, s\}$, let $z^i \in \{0, 1\}$ be the label indicating whether solution (x^i, y^i) lies in the hyperplane (h, h_0) or not. That is, $z^i = 1$ if $\langle h, x^i \rangle = h_0$, and $z^i = 0$ otherwise. We also denote by \bar{z} the average value of the variables z^1, \dots, z^s .

The proposed training scheme for oracle $\phi_{(h, h_0)}$ is the following. First, if \bar{z} is very close to one, then the oracle always suggests adding this hyperplane to the relaxation. More precisely, if $\bar{z} \geq z^{\text{FIX}}$, where z^{FIX} is a fixed hyper-parameter, then the oracle always returns **ADD**. Next, the oracle verifies whether the labels are sufficiently balanced to perform supervised training. More precisely, if $\bar{z} \notin [z^{\text{MIN}}, z^{\text{MAX}}]$, where z^{MIN} and z^{MAX} are hyper-parameters, the oracle always returns **SKIP**. Finally, if $\bar{z} \in [z^{\text{MIN}}, z^{\text{MAX}}]$, then the algorithm constructs a binary classifier and evaluates its precision and recall on the training set using k -fold cross validation. For a definition of precision, recall and k -fold cross validation, see Alpaydin (2014). If the binary classifier proves to have sufficiently high precision and recall, the oracle returns its predictions during the test phase. Otherwise, the oracle discards the binary classifier and always returns **SKIP** instead. The minimum acceptable recall is given by a fixed hyperparameter α^R . The minimum acceptable precision is computed by the expression

$$\max\{\bar{z}, 1 - \bar{z}\} \cdot (1 - \alpha^P) + \alpha^P,$$

where α^P is a hyper-parameter. Intuitively, the oracle only accepts the trained binary classifier if it significantly outperforms a dummy classifier which always returns the same label for every input. When $\alpha^P = 0$, the trained binary classifier is acceptable as long as it has same precision as the dummy classifier. When $\alpha^P = 1$, the classifier is only acceptable if it has perfect precision.

Table 1 shows the precise hyper-parameters used in our experiments, for each type of hyperplane. Due to the high dimensionality of the parameters, we do not train the binary classifiers directly the original vector of parameters p . Instead, we propose using as training features only the following subset of parameters: the peak system load, the hourly system loads, the average production cost of generator g and the average production costs of the remaining generators. We propose the usage of support vector machines (with linear kernels), since, in our experiments, these models performed better than logistic regression and random

decision forests models, while remaining computationally friendly. Neural networks were not considered given the small number of training samples available.

Table 1. Hyper-parameters for affine subspace detection oracle.

Hyperplane	z^{FIX}	z^{MIN}	z^{MAX}	α^{R}	α^{P}
$x_{gt} = 0$	1.000	0.250	0.750	0.90	0.90
$x_{gt} = 1$	1.000	0.250	0.750	0.75	0.75
$x_{gt} = x_{g,t+1}$	0.975	0.025	0.975	0.50	0.50

Unlike the previous two oracles, the affine subspace oracle described in this subsection requires a substantial number of samples in order to give reliable predictions, making it less suitable for online learning.

4 Computational Experiments

In this section we evaluate the practical impact of the ML oracles introduced in Section 3 by performing extensive computational experiments on a diverse set of large-scale and realistic SCUC instances.

4.1 Computational Environment and Instances

The three proposed machine-learning oracles were implemented in Python 3, using `pandas` and `scikit-learn`. IBM ILOG CPLEX 12.8.0 was used as a MIP solver. The code responsible for constructing the MIP model, querying the oracles and translating the given hints into instructions for CPLEX was written in Java, using ILOG Concert Technology. Websockets were used for the communication between the Java and the Python portions of the code. The training instances were generated and solved to optimality on a single node of the Bebop cluster at Argonne National Laboratory (Intel Xeon E5-2695v4, 36 cores, 128GB DDR4). During the training phase, CPLEX was configured to run in single-threaded mode and multiple training instances were solved in parallel at a time. To accurately measure the running times during the test phase, a dedicated node at the same cluster was used, and only a single test instance was solved at a time. During this phase, CPLEX was configured to use 8 cores.

A total of eight realistic instances from MATPOWER (Zimmerman et al., 2011) were selected to evaluate the effectiveness of the method. These instances correspond to realistic,

Table 2. Size of selected instances.

Instance	Buses	Units	Lines
case1888rte	1,888	297	2,531
case1951rte	1,951	391	2,596
case2848rte	2,848	547	3,776
case3012wp	3,012	502	3,572
case3375wp	3,374	596	4,161
case6468rte	6,468	1,295	9,000
case6470rte	6,470	1,330	9,005
case6495rte	6,495	1,372	9,019
case6515rte	6,515	1,388	9,037

large-scale European test systems. Table 2 presents their main characteristics, including the number of buses, units and transmission lines. Some generator data necessary for SCUC was missing in these instances, and was artificially generated based on publicly available data from PJM (2018) and MISO (2018).

4.2 Training and Test Samples

During training, 300 variations of each of the original instances were generated and solved to optimality. We considered four sources of uncertainty: i) uncertain production and startup costs; ii) uncertain geographical load distribution; iii) uncertain peak system load; and iv) uncertain temporal load profile. The precise randomization scheme is described below. The specific parameters were chosen based on our analysis of publicly available bid and hourly demand data from PJM (2018), corresponding to the month of January, 2017.

- (i) **Production and startup costs.** In the original instances, the production cost for each generator $g \in G$ is modelled as a convex piecewise-linear function described by the parameters c_g^0 , the cost of producing the minimum amount of power, and c_g^1, \dots, c_g^k , the costs of producing each additional MW of power within the piecewise interval k . In addition, each generator has a startup cost c_g^s . In our data analysis, we observed that the daily changes in bid prices rarely exceeded $\pm 5\%$. Therefore, random numbers α_g were independently drawn from the uniform distribution in the interval $[0.95, 1.05]$, for each generator $g \in G$, and the costs of g were linearly scaled by this factor. That is, the costs for generator g were set to $\alpha_g c_g^0, \alpha_g c_g^1, \dots, \alpha_g c_g^k, \alpha_g c_g^s$.
- (ii) **Geographical load distribution.** In the original instances, each bus $b \in B$ is responsible for a certain percentage d_b of the total system load. To generate variations of

these parameters, random numbers β_b were independently drawn from the uniform distribution in the interval $[0.90, 1.10]$. The percentages d_b were then linearly scaled by the β_b factors and later normalized. More precisely, the demand for each bus $b \in B$ was set to $\frac{\beta_b d_b}{\sum_{i \in B} \beta_i}$.

(iii) **Peak system load and temporal load profile.** For simplicity, assume $T = \{1, \dots, 24\}$.

Let D_1, \dots, D_{24} denote the system-wide load during each hour of operation, and let $\gamma_t = \frac{D_{t+1}}{D_t}$ for $t = 1, \dots, 23$, be the hourly variation in system load. In order to generate realistic distribution for these parameters, we analyzed hourly demand data from PJM (2018). More specifically, we computed the mean μ_t and variance σ_t^2 of each parameter γ_t , for $t = 1, \dots, 23$. To generate instance variations, random numbers γ'_t were then independently drawn from the Gaussian distribution $N(\mu_t, \sigma_t^2)$. Note that the γ' parameters only specify the variation in system load from hour to hour, and are not sufficient to determine D_1, \dots, D_{24} . Therefore, in addition to these parameters, a random number ρ , corresponding to the peak system load $\max\{D_1, \dots, D_{24}\}$, was also generated. In the original instances, the peak system load is always 60% of the total capacity. Based on our data analysis, we observed that the actual peak load rarely deviates more than $\pm 7.5\%$ from the day-ahead forecast. Therefore, to generate instance variations, ρ was sampled from the uniform distribution in the interval $[0.6 \times 0.925C, 0.6 \times 1.075C]$, where C is the total capacity. Note that the ρ and γ' parameters are now sufficient to construct D_1, \dots, D_{24} . Figure 1 shows a sample of some artificially generated load profiles.

During test, 50 additional variations of each original instance were generated, using the same randomization scheme outline above, but with a different random seed. These instances were then solved to optimality using four different strategies: without any machine-learning (**zero**), using only the transmission oracle (**tr**), using transmission and warm-start oracles (**tr-ws**) and finally using only the transmission and affine subspace detection oracles (**tr-aff**). For strategies **zero**, **tr** and **tr-ws**, CPLEX was configured to use a relative MIP gap tolerance of 0.1%. For strategy **tr-aff**, this tolerance was reduced to 0.05%, to compensate for eventual inaccurate predictions.

4.3 Performance evaluation

We start by evaluating the performance of the transmission oracle. Table 3 shows the average number of transmission and N-1 security constraints added to the relaxation per time period for each instance, as well as the average number of iterations required by Algorithm 1 to converge. Column **zero** corresponds to the case where no machine learning is used, while

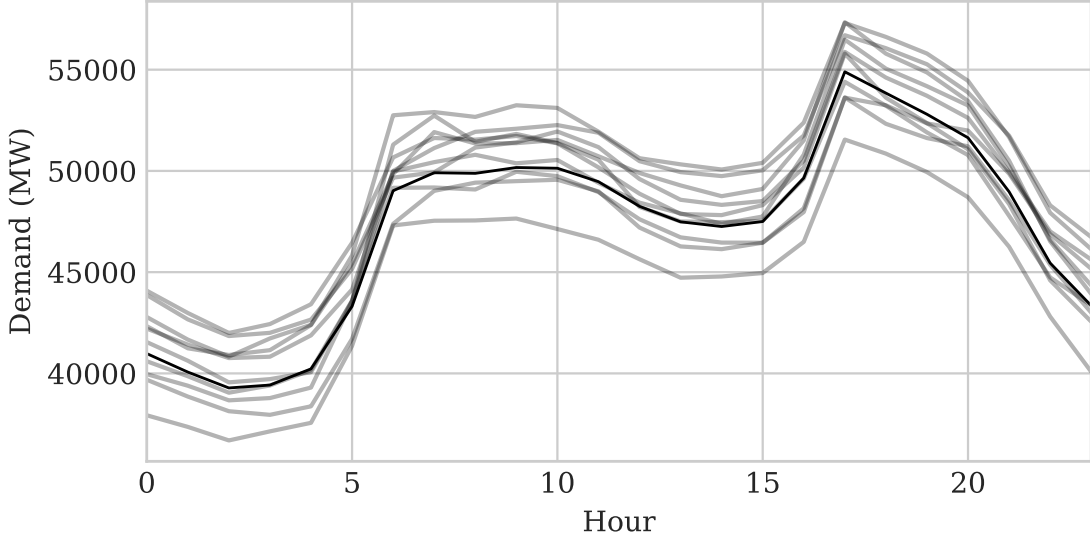


Fig. 1. Sample of artificially generated load profiles.

column \mathbf{tr} correponds to the case where the oracle described in Subsection 3.1 is employed. We observe that the transmission oracle was very effective at bringing the number of iterations down. In fact, for the vast majority of the test cases, the algorithm terminated after one iteration, which indicates that the oracle was able to correctly identify a superset of the required constraints. We also observe that this superset of constraints was only slightly larger than the set obtained without machine learning. Based on these results, we conclude that the very simple learning strategy presented in Subsection 3.1 is already sufficiently good. Even if more elaborate strategies were able to bring the number of added constraints down without increasing the average number of iterations, we would only expect very minor performance improvements.

Next, we evaluate the performance of the affine subspace detection oracle. For each instance, Table 4 shows the total number of commitment variables in the formulation, the percentage of commitment variables x_{gt} fixed to zero, fixed to one, fixed to the next time period (that is, $x_{gt} = x_{g,t+1}$), as well as the percentage of commitment variables left free. As explained in Subsection 3.3, each variable is fixed to at most one value, and therefore the percentages sum to 100%. We observe that the affine oracle is able to fix a large number of commitment variables, for instances of all sizes. On average, the oracle was able to eliminate 94% of the variables, leaving only 6% free, a considerable reduction in problem size. To evaluate the accuracy of such variable fixing decisions, we compared the recommendations provided by the oracle against an optimal solution obtained by the MIP solver (without

Table 3. Average number of iterations and transmission constraints added per time period, with machine learning (tr) and without (zero).

Instance	zero		tr	
	Constraints	Iterations	Constraints	Iterations
<code>case1888rte</code>	12.10	5.16	24.00	1.00
<code>case1951rte</code>	2.60	3.08	7.00	1.00
<code>case2848rte</code>	4.56	3.50	7.36	1.02
<code>case3012wp</code>	8.90	4.18	21.02	1.02
<code>case3375wp</code>	7.42	4.28	20.00	1.00
<code>case6468rte</code>	19.64	6.92	32.00	1.00
<code>case6470rte</code>	11.32	5.22	17.00	1.00
<code>case6495rte</code>	17.68	6.62	28.00	1.00
<code>case6515rte</code>	14.58	5.48	16.00	1.00
Average	10.98	4.94	19.15	1.00

machine learning). We note that such a comparison is not entirely fair to the oracle, since a large number of optimal solutions exist within the 0.1% optimality gap threshold. These solutions have slight variations, and disagree with each other in a number of commitment variables. Nevertheless, on average, 99.8% of the hints provided by the oracle agreed the optimal solution obtained by CPLEX.

Table 4. Total number of commitment variables; percentage of fixed variables by affine oracle and percentage of correctly-identified hyperplanes.

Instance	Commitment Variables					
	Total	Fix Zero	Fix One	Fix Next	Free	Precision
<code>case1888rte</code>	7128.0	17.9%	52.0%	24.7%	5.4%	99.8%
<code>case1951rte</code>	9384.0	20.0%	45.9%	27.8%	6.3%	99.8%
<code>case2848rte</code>	13128.0	23.9%	44.8%	23.2%	8.2%	99.7%
<code>case3012wp</code>	12048.0	18.5%	54.5%	21.3%	5.6%	99.8%
<code>case3375wp</code>	14304.0	14.4%	57.8%	22.4%	5.5%	99.8%
<code>case6468rte</code>	31080.0	7.6%	72.4%	12.8%	7.2%	99.9%
<code>case6470rte</code>	31920.0	7.3%	70.3%	16.2%	6.2%	99.8%
<code>case6495rte</code>	32928.0	5.8%	75.4%	13.1%	5.7%	99.9%
<code>case6515rte</code>	33312.0	6.1%	75.5%	12.0%	6.4%	99.9%
Average	20581.3	13.5%	60.9%	19.3%	6.3%	99.8%

Next, we evaluate what impact of the previous oracles on total running time. Table 5 shows the average MIP running time (in seconds) necessary to solve the 50 variations of each

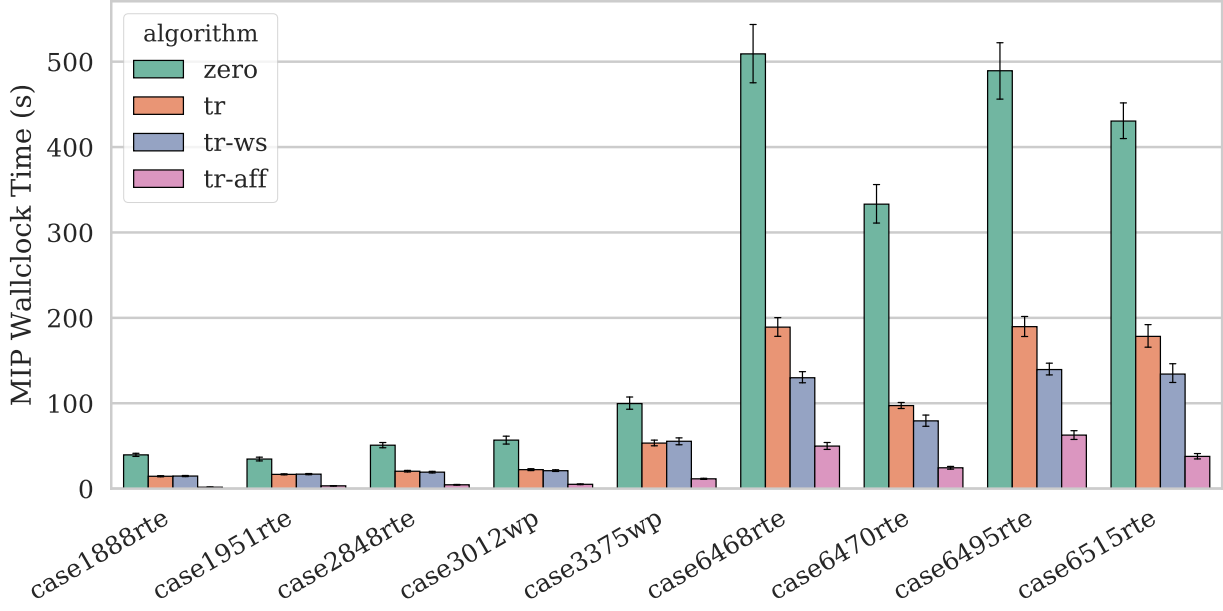
instance. Four different strategies are presented: no machine learning (**zero**), using only the transmission oracle (**tr**), using transmission and warm-start oracles (**tr-ws**) and finally using only the transmission and affine subspace detection oracles (**tr-aff**). Figure 2 shows the same results in graphical form, along with error bars representing 95% confidence intervals.

Table 5. Impact of machine-learning oracles on running-time and solution quality.

Instance	zero		tr		tr-ws		tr-aff	
	Time	Time	Speedup	Time	Speedup	Time	Speedup	Time
case1888rte	39.5	14.5	2.7x	14.7	2.7x	1.7	23.5x	
case1951rte	34.6	16.7	2.1x	17.0	2.0x	3.3	10.6x	
case2848rte	50.9	20.4	2.5x	19.3	2.6x	4.5	11.3x	
case3012wp	56.8	22.2	2.6x	21.0	2.7x	5.1	11.2x	
case3375wp	99.6	53.3	1.9x	55.5	1.8x	11.5	8.7x	
case6468rte	509.1	189.1	2.7x	129.9	3.9x	49.8	10.2x	
case6470rte	333.1	97.3	3.4x	79.4	4.2x	24.4	13.6x	
case6495rte	489.4	189.7	2.6x	139.5	3.5x	62.7	7.8x	
case6515rte	430.5	178.3	2.4x	134.2	3.2x	37.8	11.4x	
Average	227.1	86.8	2.5x	67.8	3.0x	22.3	12.0x	

Without any machine learning, the instances were solved on average in 227 seconds of computational time. By using the transmission oracle, a 2.5x speedup was achieved, bringing the average running time down to 86 seconds. This is already a very considerable speedup, obtained with a very simple learning strategy. Using the MIP start oracle in conjunction with the transmission oracle resulted in a slightly improved speedup of 3.0x, with an average running time of 68 seconds. We note that the MIP start oracle only proved beneficial for the larger instances, composed by more than 6000 buses. Finally, by using the affine subspace detection oracle in conjunction with the transmission oracle, we obtained the considerably better speedup of 12.0x, on average, bringing the total running time down to only 22 seconds. Unlike the MIP start oracle, the affine subspace oracle was very helpful for instances of all sizes.

Besides the improvements in average running times, another benefit of strategy **tr-aff** was a significant reduction in the *variability* of these running times, especially for larger instances. This can be inferred from the error bars in Figure 2. For example, without any machine learning, instance **case6468** presented standard deviation of 118 seconds. Assuming a normal distribution, this implies that a running time of 746 seconds (two standard deviations away from the mean) would not be atypical. In comparison, for strategy **tr-aff**, the standard

Fig. 2. Running time.

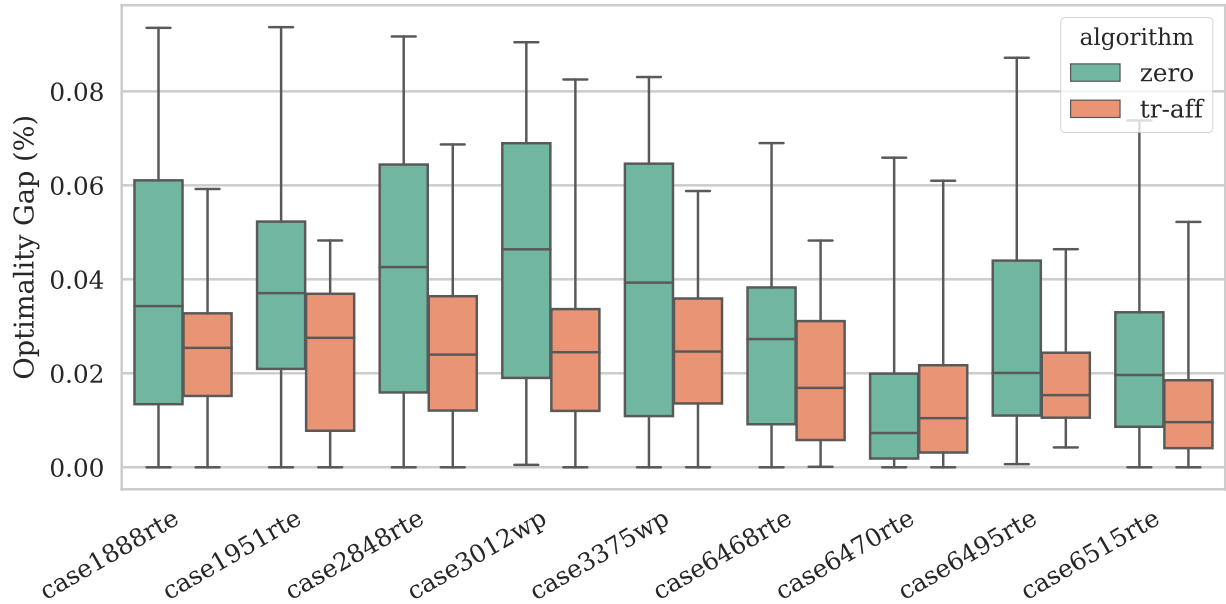
deviation was only 14 seconds. Repeating the same analysis, we see that typical running times stay below 89 seconds.

Besides the combinations shown in the table, we also performed computational experiments using the MIP start oracle alone (strategy `ws`), and all three oracles combined (strategy `tr-ws-aff`). In general, strategies `ws` and `tr-ws-aff` did not perform any better than strategies `zero` and `tr-aff`, respectively.

Finally, we evaluate the impact of the affine subspace oracle in the objective values of the solutions. As explained in Subsection 3.3, we recall that the affine oracle could potentially lead to suboptimal solutions by fixing too many commitment variables to incorrect values. To show that this is not the case, we solved each of the instance variation to 0.01% optimality and compared this objective value to the objective values produced by strategies `zero` and `tr-aff`. Figure 3 shows a box plot of the optimality gaps obtained. We observe that, for all instances and variations, strategy `tr-aff` stayed below the 0.1% optimality gap threshold, which indicates that all solutions obtained by this strategy were optimal.

5 Conclusion

In this work, we described how to significantly expedite the solution of the Security-Constrained Unit Commitment Problem by using simple machine learning techniques. More

Fig. 3. Optimality gap.

specifically, by predicting redundant constraints, good initial feasible solutions and affine subspaces, we were able to achieve 12x speedup on average in a diverse set of realistic and large-scale SCUC instances, without any negative impact on solution quality. The techniques presented can also be readily adapted to other challenging combinatorial problems.

Acknowledgments This material is based upon work supported by Laboratory Directed Research and Development (LDRD) funding from Argonne National Laboratory, provided by the Director, Office of Science, of the U.S. Department of Energy under Contract No. DE-AC02-06CH11357. We gratefully acknowledge use of the Bebop cluster in the Laboratory Computing Resource Center at Argonne National Laboratory.

Appendix

Here we present the complete MIP formulation that was used to during the computational experiments in Section 4. Consider a power system composed by a set B of buses, a set G of generators and a set L of transmission lines. Furthermore, let $T = \{1, \dots, 24\}$ be the set of hours within the planning horizon, and let G_b be the set of generators located at bus b . Let d_{bt} be the demand (in MWh) from bus b at time t . We recall that each generator $g \in G$ has a convex production cost curve, modeled as a piecewise-linear function with a set K of segments. For each generator $g \in G$, define the following constants:

- c_g^0 , cost of keeping generator operational for one hour, producing at its minimum output level.
- c_g^k , cost to produce each additional MWh of power, for each segment $k \in K$.

- c_g^S , cost to start the generator up.
- P_g^k , amount of power available (in MWh) in segment $k \in K$.
- RU_g , maximum allowed rise in production (in MWh) from one hour to the next.
- RD_g , maximum allowed drop in production (in MWh) from one hour to the next.
- P_g^{\min} , minimum amount of power (in MWh) the generator must produce if it is operational.
- P_g^{\max} , maximum amount of power (in MWh) the generator can produce.
- UT_g , minimum amount of time (in hours) the generator must stay operational after being switched on.
- DT_g , minimum amount of time (in hours) the generator must stay offline after being switched off.

For each transmission line $l \in L$, let F_l^0 be its flow limit (in MWh) under normal conditions and F_l^c be its flow limit when there is an outage on line $c \in L$. Similarly, let δ_{lb}^0 and δ_{lb}^c be, respectibely, the injection shift factors for line l and bus b under normal conditions, and under outage on line c .

As mentioned in Section 2, the main decision variables for this problem are $x_{gt} \in \{0, 1\}$, which indicates whether generator g is operational at time t ; and $y_{gt} \geq 0$, which indicates how much power (in MWh) generator g produces during time t . Other auxiliary variables are $z_{gt}, w_{gt} \in \{0, 1\}$ which indicate, respectively, whether generator g is started up or shut down at time t . We also define the variables y_{gt}^k which indicate how much power produced by generator g at time t comes from segment $k \in K$. Finally, let $r_{gt} \geq 0$ be a decision variable indicating the amount of reserve (in MWh) provided by generator g at time t , and let R_t be the minimum amount of system-wide reserve required at time t . Reserves are generation capacities kept aside to compensate for small load variations. Given these variables and constants, SCUC is formulated as a cost minimization problem as below:

$$\text{Minimize} \quad \sum_{g \in G} \sum_{t \in T} \left[c_g^S z_{gt} + c_g^0 x_{gt} + \sum_{k \in K} c_g^k y_{gt}^k \right] \quad (11)$$

$$\text{Subject to} \quad \sum_{g \in G} y_{gt} = \sum_{b \in B} d_{bt} \quad \forall t \in T \quad (12)$$

$$\sum_{g \in G} r_{gt} \geq R_t \quad \forall t \in T \quad (13)$$

$$\begin{aligned} \sum_{k \in K} y_{gt}^k + r_{gt} &\leq (P_g^{\max} - P_g^{\min}) x_{gt} \\ &\quad - (P_g^{\max} - RU_g) z_{gt} \\ &\quad - (P_g^{\max} - RD_g) w_{g,t+1} \end{aligned} \quad \forall g \in G, t \in \{1, \dots, 23\} : UT_g > 1 \quad (14)$$

$$\begin{aligned} \sum_{k \in K} y_{gt}^k + r_{gt} &\leq (P_g^{\max} - P_g^{\min}) x_{gt} \\ &\quad - (P_g^{\max} - RU_g) z_{gt} \\ &\quad - \max\{RU_g - RD_g, 0\} w_{g,t+1} \end{aligned} \quad \forall g \in G, t \in \{1, \dots, 23\} : UT_g = 1 \quad (15)$$

$$\begin{aligned} \sum_{k \in K} y_{gt}^k + r_{gt} &\leq (P_g^{\max} - P_g^{\min}) x_{gt} \\ &\quad - (P_g^{\max} - RD_g) w_{g,t+1} \\ &\quad - \max\{RD_g - RU_g, 0\} z_{gt} \end{aligned} \quad \forall g \in G, t \in \{1, \dots, 23\} : UT_g = 1 \quad (16)$$

$$\begin{aligned} \sum_{k \in K} y_{g,24}^k + r_{g,24} &\leq (P_g^{\max} - P_g^{\min}) x_{g,24} \\ &\quad - (P_g^{\max} - RU_g) z_{t,24} \end{aligned} \quad \forall g \in G \quad (17)$$

$$y_{gt} \leq y_{g,t-1} + RU_g \quad \forall g \in G, t \in \{2, \dots, 24\} \quad (18)$$

$$y_{gt} \geq y_{g,t-1} - RD_g \quad \forall g \in G, t \in \{2, \dots, 24\} \quad (19)$$

$$\sum_{i=\max\{1, t-UT_g+1\}}^t z_{gi} \leq x_{gt} \quad \forall t \in T, g \in G \quad (20)$$

$$\sum_{i=\max\{1, t-DT_g+1\}}^t z_{gi} \leq 1 - x_{\max\{1, t-DT_g\}, g} \quad \forall t \in T, g \in G \quad (21)$$

$$-F_l^0 \leq \sum_{b \in B} \delta_{lb}^0 \left(\sum_{g \in G_b} y_{gt} - d_{bt} \right) \leq F_l^0 \quad \forall l \in L, t \in T \quad (22)$$

$$-F_l^c \leq \sum_{b \in B} \delta_{lb}^c \left(\sum_{g \in G_b} y_{gt} - d_{bt} \right) \leq F_l^c \quad \forall c \in L, l \in L, t \in T \quad (23)$$

$$y_{gt}^k \leq P_g^k \quad \forall k \in K, g \in G, t \in T \quad (24)$$

$$y_{gt} = P_g^{\min} x_{gt} + \sum_{k \in K} y_{gt}^k \quad \forall t \in T \quad (25)$$

$$x_{gt} - x_{g,t-1} = z_{gt} - w_{gt} \quad \forall g \in G, t \in \{2, \dots, 24\} \quad (26)$$

$$x_{gt}, z_{gt}, w_{gt} \in \{0, 1\} \quad \forall g \in G, t \in T \quad (27)$$

$$r_{gt}, y_{gt}, y_{gt}^k \geq 0 \quad \forall k \in K, g \in G, t \in T \quad (28)$$

The objective function (11) includes start-up and production costs. Although start-up costs are sometimes modeled as a stepwise function of off-time, in our test they are modeled as constants. Equation (12) enforces that the total power supply equals total load. Equation (13) enforces a sufficient amount of reserve at each time period. Equations (14) to (17) enforce the production limits. Equations (18) and (19) enforce the ramping requirements. Equations (20) and (21) guarantee that, once a generator is started or shutdown, it must remain online or offline for a certain amount of time. Equations (22) and (23) require that the power flow on each transmission line does not exceed its thermal limits. Equations (24) and (25) link the variables y_{gt} and y_{gt}^k . Finally, Equation (26) link x_{gt} , z_{gt} and w_{gt} .

Bibliography

Alpaydin, E. (2014). *Introduction to machine learning*. MIT press.

Alvarez, A. M., Louveaux, Q., and Wehenkel, L. (2017). A machine learning-based approximation of strong branching. *INFORMS Journal on Computing*, 29(1):185–195.

Alvarez, A. M., Wehenkel, L., and Louveaux, Q. (2014). Machine learning to balance the load in parallel branch-and-bound.

Ardakani, A. J. and Bouffard, F. (2015). Acceleration of umbrella constraint discovery in generation scheduling problems. *IEEE Transactions on Power Systems*, 30(4):2100–2109.

Atakan, S., Lulli, G., and Sen, S. (2018). A state transition MIP formulation for the unit commitment problem. *IEEE Transactions on Power Systems*, 33(1):736–748.

Batut, J. and Renaud, A. (1992). Daily generation scheduling optimization with transmission constraints: a new class of algorithms. *IEEE Transactions on Power Systems*, 7(3):982–989.

Bouffard, F., Galiana, F. D., and Arroyo, J. M. (2005). Umbrella contingencies in security-constrained optimal power flow. In *15th Power systems computation conference, PSCC*, volume 5.

Burns, R. and Gibson, C. (1975). Optimization of priority lists for a unit commitment program. In *Proc. IEEE Power Eng. Soc. Summer Meeting, 1975*.

Chen, Y., Casto, A., Wang, F., Wang, Q., Wang, X., and Wan, J. (2016). Improving large scale day-ahead security constrained unit commitment performance. *IEEE Transactions on Power Systems*, 31(6):4732–4743.

Cohen, A. I. and Sherkat, V. R. (1987). Optimization-based methods for operations scheduling. *Proceedings of the IEEE*, 75(12):1574–1591.

Damci-Kurt, P., Küçükyavuz, S., Rajan, D., and Atamtürk, A. (2016). A polyhedral study of production ramping. *Mathematical Programming*, 158(1-2):175–205.

EIA (2018). U.S. Energy Information Administration. Wholesale Electricity and Natural Gas Market Data. <https://www.eia.gov/electricity/wholesale>. Accessed: September 27, 2018.

Feizollahi, M. J., Costley, M., Ahmed, S., and Grijalva, S. (2015). Large-scale decentralized unit commitment. *International Journal of Electrical Power & Energy Systems*, 73:97–106.

Fischetti, M., Glover, F., and Lodi, A. (2005). The feasibility pump. *Mathematical Programming*, 104(1):91–104.

Garver, L. L. (1962). Power generation scheduling by integer programming-development of theory. *Transactions of the American Institute of Electrical Engineers. Part III: Power Apparatus and Systems*, 81(3):730–734.

Gentile, C., Morales-España, G., and Ramos, A. (2017). A tight mip formulation of the unit commitment problem with start-up and shut-down constraints. *EURO Journal on Computational Optimization*, 5(1-2):177–201.

Juste, K., Kita, H., Tanaka, E., and Hasegawa, J. (1999). An evolutionary programming solution to the unit commitment problem. *IEEE Transactions on Power Systems*, 14(4):1452–1459.

Khalil, E. B., Dilkina, B., Nemhauser, G. L., Ahmed, S., and Shao, Y. (2017). Learning to run heuristics in tree search. In *26th International Joint Conference on Artificial Intelligence (IJCAI)*.

Khalil, E. B., Le Bodic, P., Song, L., Nemhauser, G. L., and Dilkina, B. N. (2016). Learning to branch in mixed integer programming. In *AAAI*, pages 724–731.

Kim, K., Botterud, A., and Qiu, F. (2018). Temporal decomposition for improved unit commitment in power system production cost modeling. *IEEE Transactions on Power Systems*, 33(5):5276–5287.

Knueven, B., Ostrowski, J., and Watson, J.-P. (2018). On mixed integer programming formulations for the unit commitment problem. Pre-print available at http://www.optimization-online.org/DB_HTML/2018/11/6930.html.

Lee, J., Leung, J., and Margot, F. (2004). Min-up/min-down polytopes. *Discrete Optimization*, 1(1):77–85.

Liang, R.-H. and Kang, F.-C. (2000). Thermal generating unit commitment using an extended mean field annealing neural network. *IEE Proceedings-Generation, Transmission and Distribution*, 147(3):164–170.

Lodi, A. and Zarpellon, G. (2017). On learning and branching: a survey. *TOP*, 25(2):207–236.

Lowery, P. (1966). Generating unit commitment by dynamic programming. *IEEE Transactions on Power Apparatus and Systems*, (5):422–426.

Merlin, A. and Sandrin, P. (1983). A new method for unit commitment at electricite de france. *IEEE Power Engineering Review*, (5):38–39.

MISO (2018). Energy Market Data. <https://www.misoenergy.org/markets-and-operations/market-reports>. Accessed December 14, 2018.

Morales-España, G., Gentile, C., and Ramos, A. (2015). Tight mip formulations of the power-based unit commitment problem. *OR Spectrum*, 37(4):929–950.

Morales-España, G., Latorre, J. M., and Ramos, A. (2013). Tight and compact MILP formulation for the thermal unit commitment problem. *IEEE Transactions on Power Systems*, 28(4):4897–4908.

Ostrowski, J., Anjos, M. F., and Vannelli, A. (2012). Tight mixed integer linear programming formulations for the unit commitment problem. *IEEE Transactions on Power Systems*, 27(1):39–46.

Pan, K. and Guan, Y. (2016). A polyhedral study of the integrated minimum-up/-down time and ramping polytope. arXiv preprint arXiv:1604.02184.

PJM (2018). Energy Market Data. <https://www.pjm.com/markets-and-operations/energy.aspx>. Accessed December 14, 2018.

Rajan, D., Takriti, S., et al. (2005). Minimum up/down polytopes of the unit commitment problem with start-up costs. *IBM Res. Rep.*, (RC23628):W0506–050.

Sasaki, H., Watanabe, M., Kubokawa, J., Yorino, N., and Yokoyama, R. (1992). A solution method of unit commitment by artificial neural networks. *IEEE Transactions on Power Systems*, 7(3):974–981.

Shaw, J. J. (1995). A direct method for security-constrained unit commitment. *IEEE Transactions on Power Systems*, 10(3):1329–1342.

Shaw, P. (1998). Using constraint programming and local search methods to solve vehicle routing problems. In Maher, M. and Puget, J.-F., editors, *Principles and Practice of Constraint Programming — CP98*, pages 417–431, Berlin, Heidelberg. Springer Berlin Heidelberg.

Tejada-Arango, D. A., Sánchez-Martin, P., and Ramos, A. (2018). Security constrained unit commitment using line outage distribution factors. *IEEE Transactions on Power Systems*, 33(1):329–337.

Walsh, M. and O’malley, M. (1997). Augmented hopfield network for unit commitment and economic dispatch. *IEEE Transactions on Power Systems*, 12(4):1765–1774.

Wang, C. and Shahidehpour, S. (1993). Effects of ramp-rate limits on unit commitment and economic dispatch. *IEEE Transactions on Power Systems*, 8(3):1341–1350.

Xavier, A. S., Qiu, F., Wang, F., and Thimmapuram, P. R. (2019). Transmission constraint filtering in large-scale security-constrained unit commitment. *IEEE Transactions on Power Systems*, pages 1–1.

Zhai, Q., Guan, X., Cheng, J., and Wu, H. (2010). Fast identification of inactive security constraints in scuc problems. *IEEE Transactions on Power Systems*, 25(4):1946–1954.

Zimmerman, R. D., Murillo-Sánchez, C. E., and Thomas, R. J. (2011). MATPOWER: Steady-state operations, planning, and analysis tools for power systems research and education. *IEEE Transactions on power systems*, 26(1):12–19.